Supporting information for

Effects of cation vacancies at tetrahedral sites in cobalt spinel oxides on oxygen evolution catalysis

Wei Liu[a], Masao Kamiko[a], Ikuya Yamada[b], Shunsuke Yagi[a,*]

[a]Institute of Industrial Science, The University of Tokyo, 4–6–1 Komaba, Meguro-ku, Tokyo 153–8505, Japan
[b]Department of Materials Science, Graduate School of Engineering, Osaka Metropolitan University, 1-1 Gakuen-cho, Naka-ku, Sakai, Osaka 599-8531, Japan

*Corresponding author
E-mail: syagi@iis.u-tokyo.ac.jp (S. Yagi)

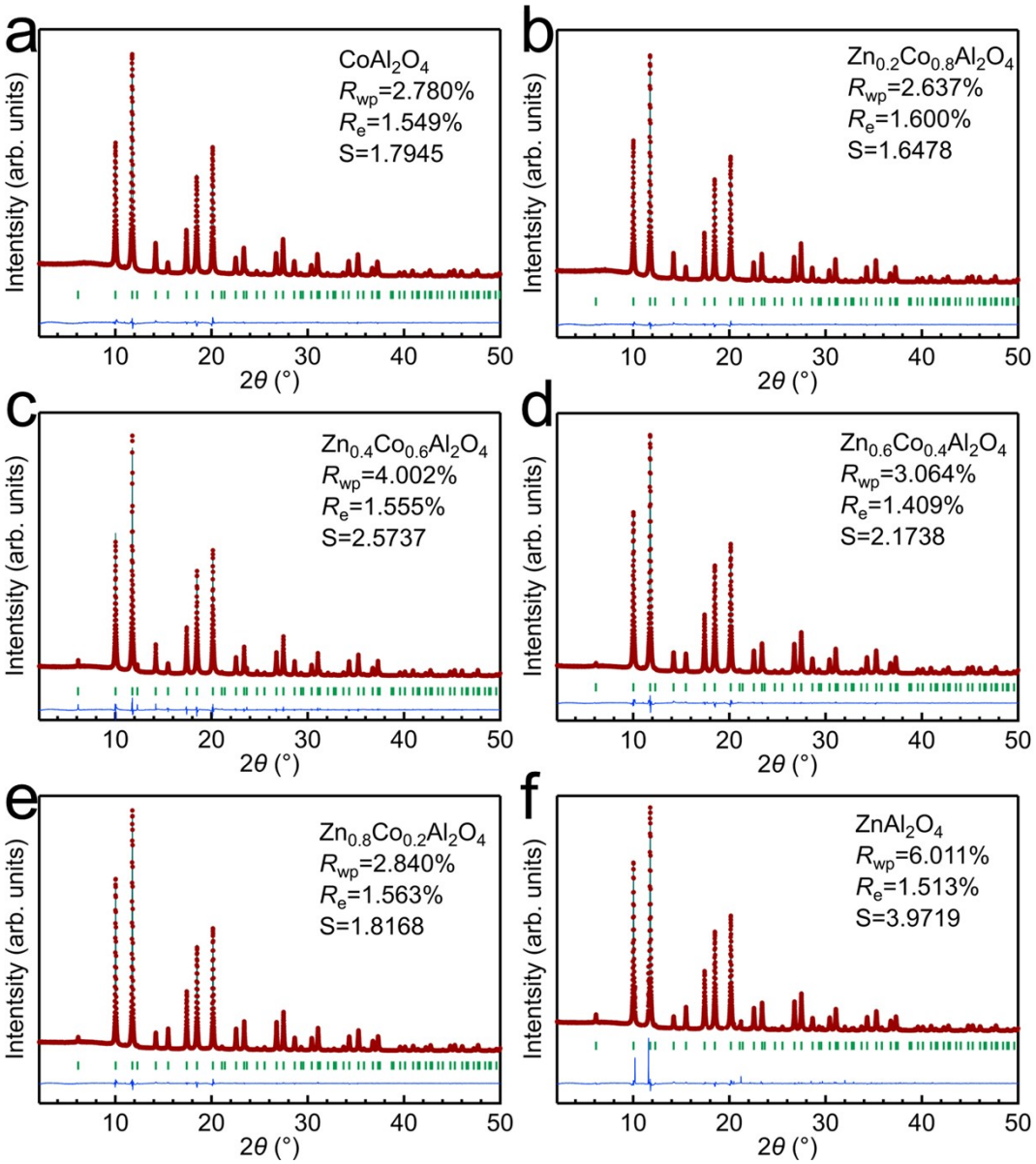

Figure S1. Synchrotron X-ray diffraction (SXRD) patterns of $Zn_xCo_{1-x}Al_2O_4$ (x = 0, 0.2, 0.4, 0.6, 0.8, and 1 in (a) to (f), respectively) and their fitting results by Rietveld refinement. The red dots indicate the observed profiles, green curves indicate the fitting curves, green bars represent the Bragg diffraction positions, and blue lines illustrate the differences between the observed profiles and fitting curves. The wavelength of the irradiated X-rays was calibrated to 0.49995 Å using a standard sample, CeO_2. R_{wp} indicates the reliability-weighted pattern factor, R_e indicates the expected reliability factor and S indicates the goodness-of-fit indicator, where $S = R_{wp}/R_e$.

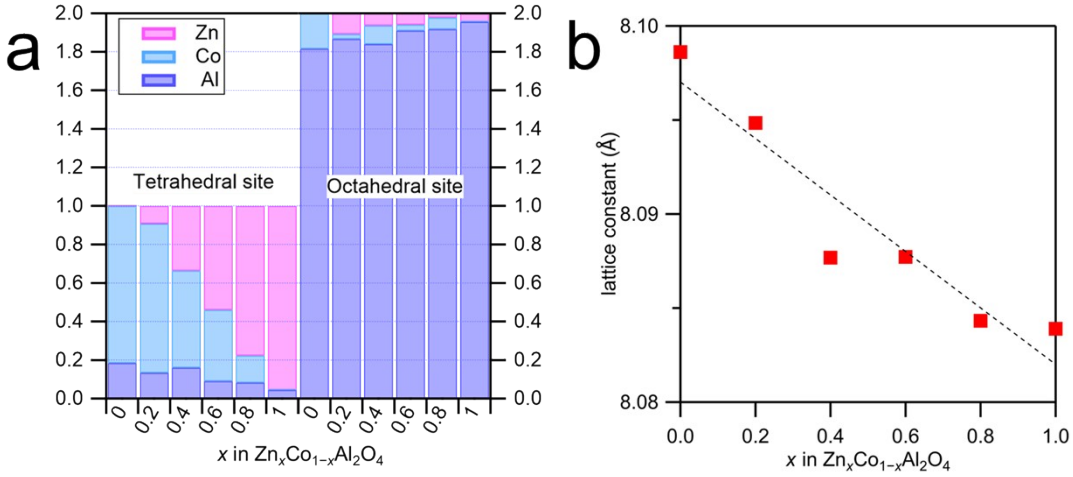

Figure S2. (a) Atomic occupancy of Zn, Co, and Al ions in $Zn_xCo_{1-x}Al_2O_4$ (x = 0, 0.2, 0.4, 0.6, 0.8, and 1). (b) Relationship between Zn substitution ratio and lattice constants obtained from Rietveld refinement of synchrotron X-ray diffraction (SXRD) patterns.

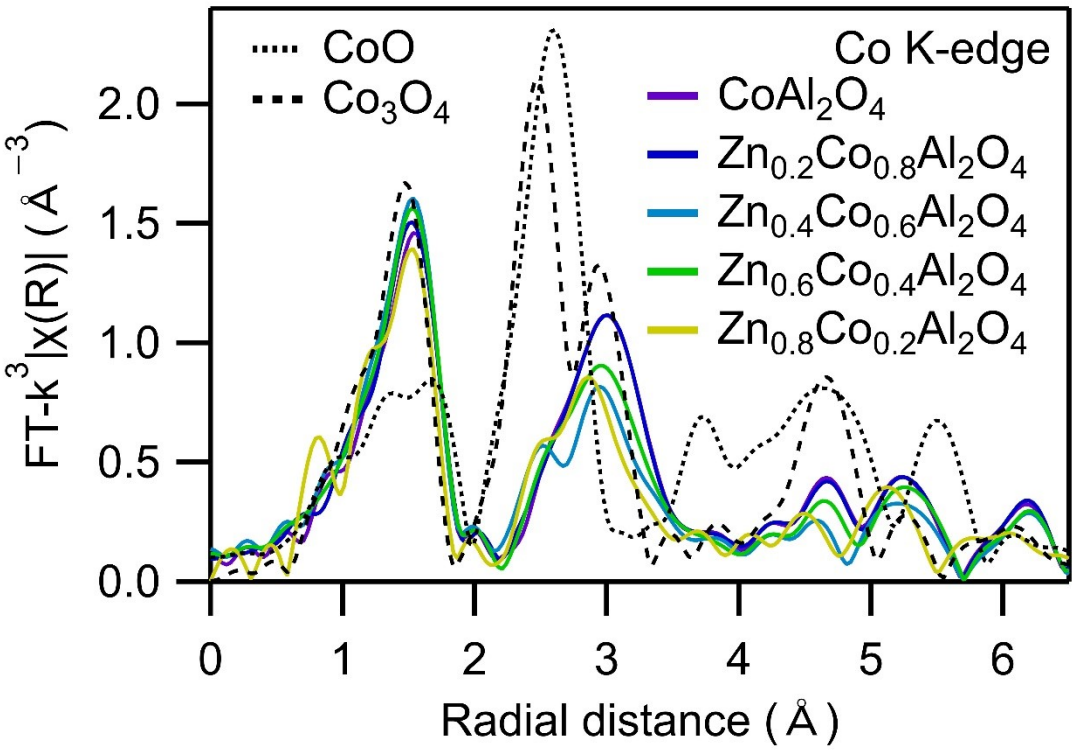

Figure S3. Fourier transformation of the Co K-edge extended X-ray absorption fine structure (EXAFS) spectra in the R space for $Zn_xCo_{1-x}Al_2O_4$ (x = 0.2, 0.4, 0.6, 0.8, and 1) with CoO and Co_3O_4 as standard references.

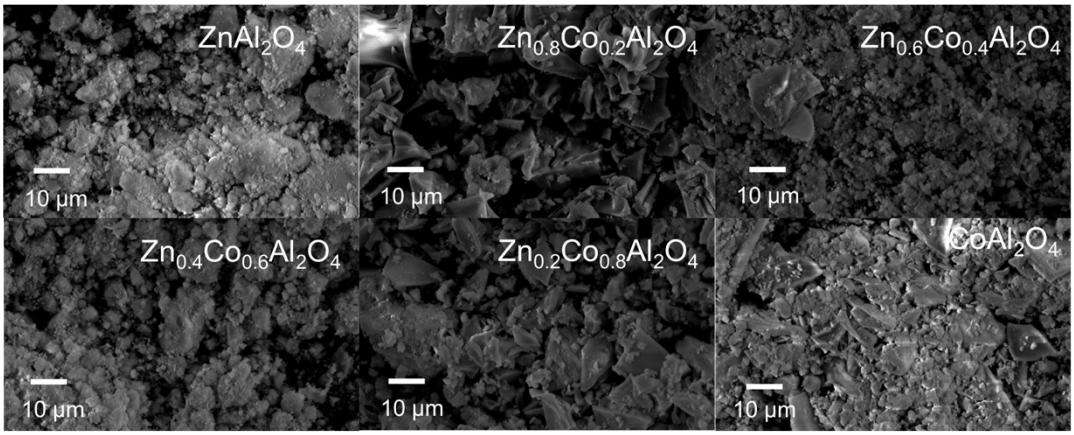

Figure S4. Scanning electron microscopy (SEM) images of $Zn_xCo_{1-x}Al_2O_4$ (x = 0, 0.2, 0.4, 0.6, 0.8, and 1) with a scale bar of 10 μm.

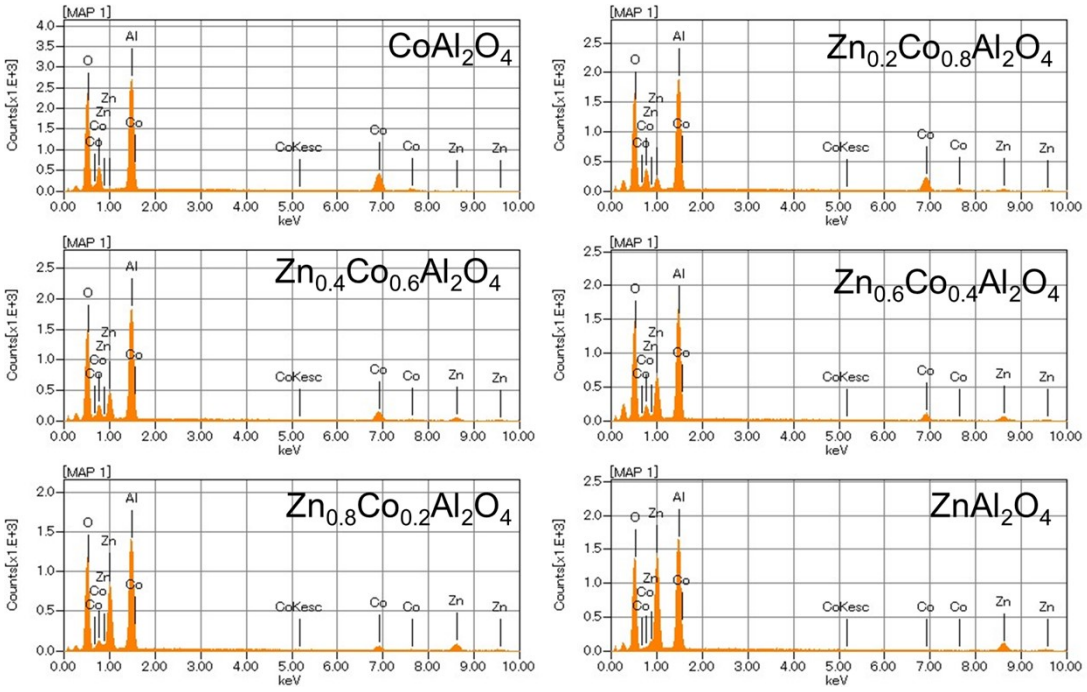

Figure S5. Elemental dispersive spectra of $Zn_xCo_{1-x}Al_2O_4$ (x = 0, 0.2, 0.4, 0.6, 0.8, and 1).

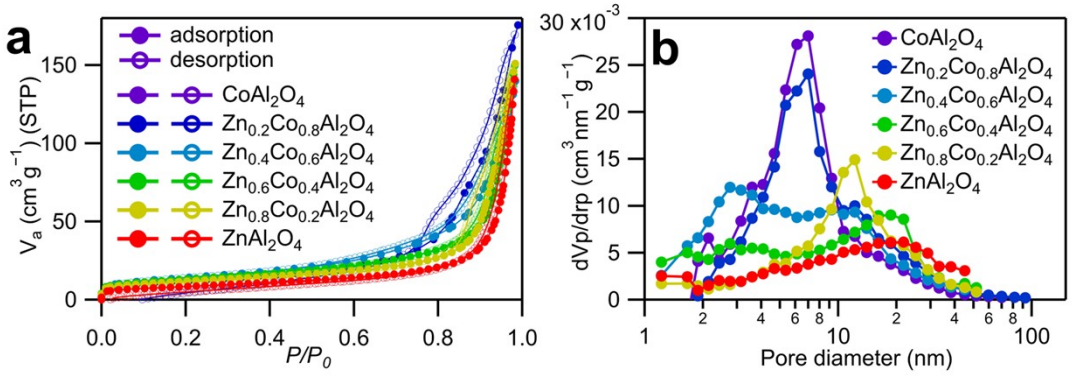

Figure S6. (a) Surface area evaluated by Brunauer–Emmett–Teller (BET) analysis of N_2 adsorption/desorption isotherms and (b) pore size distribution of $Zn_{1-x}Co_xAl_2O_4$ variants (x = 0, 0.2, 0.4, 0.6, 0.8, and 1) obtained using the Barrett–Joyner–Halenda method. STP: standard temperature and pressure. P/P_0: relative pressure to 1 atm. dVp/drp: relative ratio of pore size distribution.

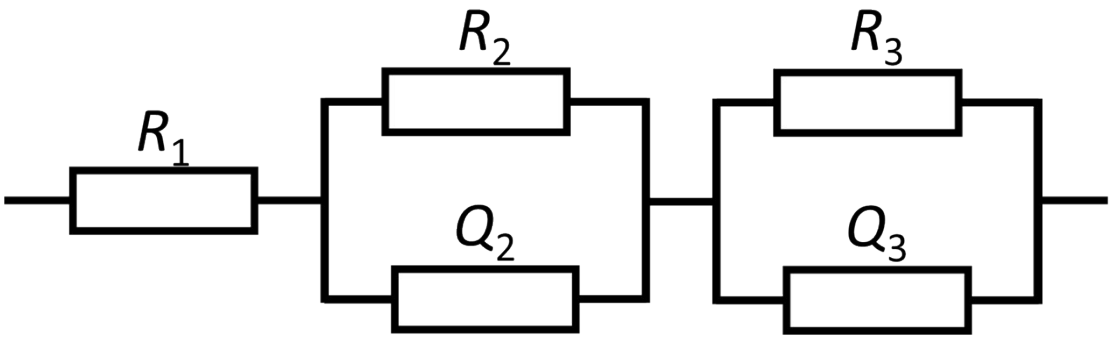

Figure S7. Equivalent circuit used for curve fitting of the electrochemical impedance spectroscopy (EIS) spectra in Fig. 2c. *R* indicates the resistances and *Q* indicates the constant phase elements.

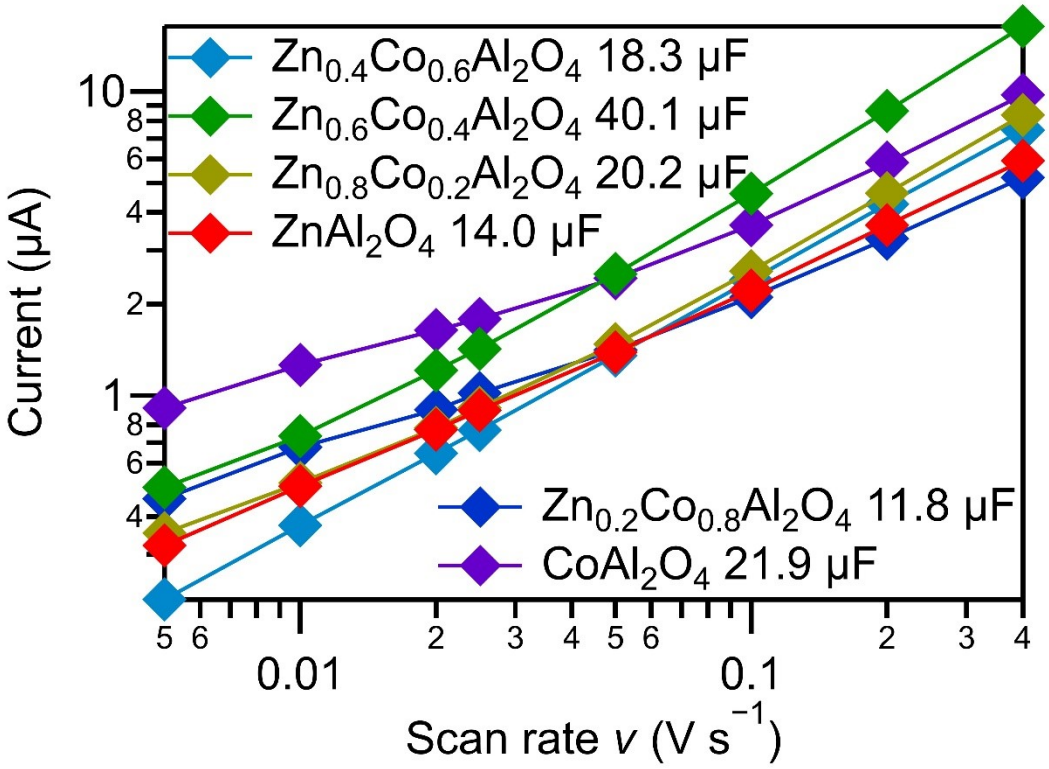

Figure S8. Double-layer capacitances for $Zn_xCo_{1-x}Al_2O_4$ (x = 0, 0.2, 0.4, 0.6, 0.8, and 1) calculated from the slopes between the currents versus different scan rates obtained from cyclic voltammetry scans between 0.876 V and 0.976 V.

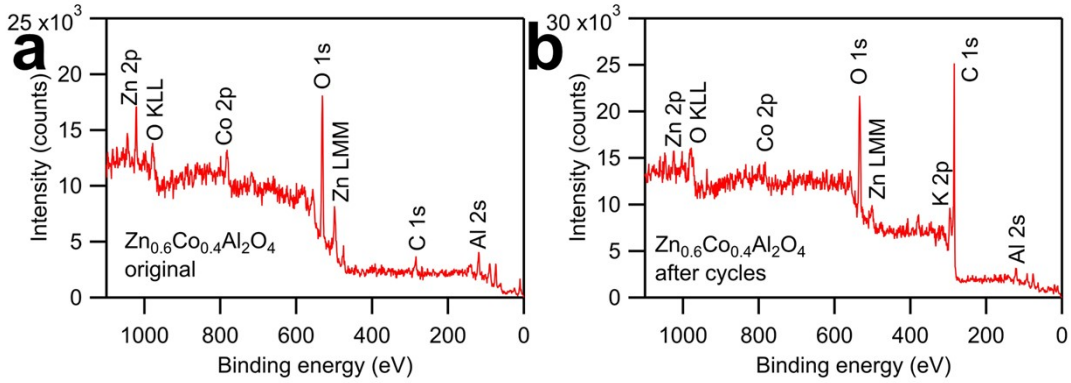

Figure S9. The wide-scan X-ray photoelectron spectroscopy (XPS) spectra for $Zn_{0.6}Co_{0.4}Al_2O_4$ before and after electrochemical tests for 1200 cycles of potential sweep from 0.926 V to 1.626 V vs. Reversible hydrogen electrode (RHE) at 10 mV s^{-1} in a 0.1 M KOH aqueous solution.

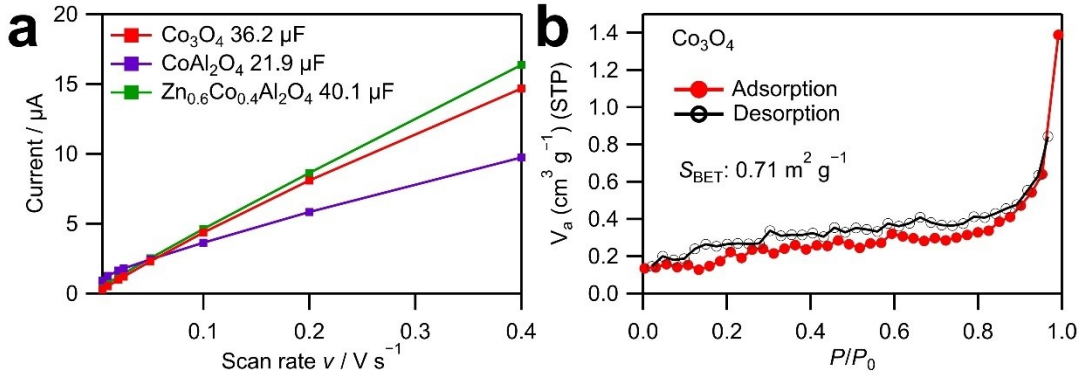

Figure S10 (a) Double-layer capacitances for Co_3O_4, $CoAl_2O_4$ and $Zn_{0.6}Co_{0.4}Al_2O_4$ calculated from the slopes between the currents versus different scan rates obtained from cyclic voltammetry scans between 0.876 V and 0.976 V. (b) Surface area evaluated by Brunauer–Emmett–Teller (BET) analysis of N_2 adsorption/desorption isotherms of Co_3O_4.

Table S1. Lattice constant (a), atomic fractional coordinates (x, y, and z), and site occupancies in $Zn_xCo_{1-x}Al_2O_4$ (x = 0–1, space group: 227, $Fd\bar{3}m$) determined by Rietveld refinement of the SXRD patterns in Fig. 1.

x	a (Å)	Atom	Site	Occupancy	x	y	z	B (Å^2)	*Reliability factors*	
0	8.09861 (9)	Co1	8*a*	0.8157 (12)	1/8	1/8	1/8	0.261 (7)	R_{wp}	2.780 %
		Al1	8*a*	0.1843	1/8	1/8	1/8	0.261	R_e	1.549 %
		Co2	16*d*	0.0921	0	0	0	0.297 (9)	*S*	1.7945
		Al2	16*d*	0.9079	0	0	0	0.297		
		O	32*e*	1	0.23632 (6)	0.23632	0.23632	0.379 (14)		
0.2	8.09484 (7)	Zn1	8*a*	0.0922 (366)	1/8	1/8	1/8	0.248 (8)	R_{wp}	2.637 %
		Co1	8*a*	0.7746 (441)	1/8	1/8	1/8	0.248	R_e	1.600 %
		Al1	8*a*	0.1332	1/8	1/8	1/8	0.248	*S*	1.6478
		Zn2	16*d*	0.0539	0	0	0	0.270 (9)		
		Co2	16*d*	0.0127	0	0	0	0.270		
		Al2	16*d*	0.9334	0	0	0	0.270		
		O	32*e*	1	0.23603 (5)	0.23603	0.23603	0.347 (15)		
0.4	8.08768 (6)	Zn1	8*a*	0.3369 (582)	1/8	1/8	1/8	0.331 (11)	R_{wp}	4.002 %
		Co1	8*a*	0.5031 (700)	1/8	1/8	1/8	0.331	R_e	1.555 %
		Al1	8*a*	0.1600	1/8	1/8	1/8	0.331	*S*	2.5737
		Zn2	16*d*	0.0316	0	0	0	0.229 (13)		
		Co2	16*d*	0.0484	0	0	0	0.229		
		Al2	16*d*	0.9200	0	0	0	0.229		
		O	32*e*	1	0.23624 (8)	0.23624	0.23624	0.503 (24)		
0.6	8.087	Zn1	8*a*	0.5403 (322)	1/8	1/8	1/8	0.232 (7)	R_{wp}	3.064 %
		Co1	8*a*	0.3691 (384)	1/8	1/8	1/8	0.232	R_e	1.409 %
		Al1	8*a*	0.0906	1/8	1/8	1/8	0.232	*S*	2.1738

		Zn2	16*d*	0.0298	0	0	0	0.263 (9)		
		Co2	16*d*	0.0155	0	0	0	0.263		
		Al2	16*d*	0.9547	0	0	0	0.263		
		O	32*e*	1	0.23607 (5)	0.23607	0.23607	0.248 (14)		
0.8	8.084 32 (6)	Zn1	8*a*	0.7774 (323)	1/8	1/8	1/8	0.227 (7)	R_{wp}	2.840 %
		Co1	8*a*	0.1404 (384)	1/8	1/8	1/8	0.227	R_e	1.563 %
		Al1	8*a*	0.0822	1/8	1/8	1/8	0.227	*S*	1.816 8
		Zn2	16*d*	0.0113	0	0	0	0.248 (9)		
		Co2	16*d*	0.0298	0	0	0	0.248		
		Al2	16*d*	0.9589	0	0	0	0.248		
		O	32*e*	1	0.23586 (5)	0.23586	0.23586	0.251 (15)		
1	8.083 90 (14)	Zn1	8*a*	0.9554 (16)	1/8	1/8	1/8	0.282 (11)	R_{wp}	6.011 %
		Al1	8*a*	0.0446	1/8	1/8	1/8	0.282	R_e	1.513 %
		Zn2	16*d*	0.0223	0	0	0	0.351 (19)	*S*	3.971 9
		Al2	16*d*	0.9777	0	0	0	0.351		
		O	32*e*	1	0.23584 (10)	0.23584	0.23584	0.158 (28)		

Note: In the fitting, the Zn/Co/Al ratio was set to the nominal value. For example, in the fitting of $Zn_{0.6}Co_{0.4}Al_2O_4$, the total amounts of Zn, Co, and Al were set as 0.6, 0.4, and 2, respectively. Certain constraint parameters were used in the fitting of $Zn_xCo_{1-x}Al_2O_4$.

A(Al1,g) = 1-A(Zn1,g)-A(Co1,g)

A(Al2,g) = 1-A(Zn2,g)-A(Co2,g)

A(Co2,g) = 0.5*(1−*x*)-0.5*A(Co1,g)

A(Zn2,g) = 0.5**x*-0.5*A(Zn1,g)

A(Co1,B) = A(Zn1,B), A(Al1,B)=A(Zn1,B)

A(Co2,B) = A(Zn2,B), A(Al2,B)=A(Zn2,B)

A(O1,y) = A(O1,x), A(O1,z)=A(O1,x)

where A indicates functions used in the refinement, O1 indicates the oxygen ions, g indicates occupancy and B indicates the Debye–Waller factor.

For the fitting of $ZnAl_2O_4$, the impurity peaks of ZnO were excluded from the fitting, except those that overlapped with the peaks of the spinel phase.

R_{wp} indicates the reliability-weighted pattern factor, R_e indicates the expected reliability factor and S indicates the goodness-of-fit indicator, where $S= R_{wp}/R_e$.

Table S2. Values of the Co K-edge absorption energy E_0 of the first shell fitting results of X-ray absorption spectroscopy (XAS) and extended X-ray absorption fine structure (EXAFS) near the Co K-edge for $Zn_xCo_{1-x}Al_2O_4$ (x = 0.2–1). The values of E_0 were acquired from those with the largest first derivative of the X-ray absorption near edge structure (XANES) spectra.

Sample	E_0 (eV)	CN	ΔE_0	σ^2	R factor	R (Å)
$CoAl_2O_4$	7715.84	4.32±0.32	1.36±1.10	0.00382	0.006	1.949
$Zn_{0.2}Co_{0.8}Al_2O_4$	7715.73	4.49±0.41	1.19±1.37	0.00404	0.009	1.946
$Zn_{0.4}Co_{0.6}Al_2O_4$	7715.74	4.53±0.32	1.87±1.03	0.00366	0.005	1.936
$Zn_{0.6}Co_{0.4}Al_2O_4$	7716.02	4.42±0.34	1.80±1.15	0.00362	0.006	1.940
$Zn_{0.8}Co_{0.2}Al_2O_4$	7716.03	4.76±0.44	1.56±1.38	0.00387	0.009	1.935

*k range: 3–13.5; R range: 1–2; CN: coordination number; S_0^2 was fixed at 0.759 for all samples according to the Co foil reference.

Table S3. Atomic concentration ratios of Zn, Co, Al and O atoms in $Zn_xCo_{1-x}Al_2O_4$ (x = 0–1) estimated by elemental dispersive spectroscopy.

Sample	Zn (%)	Co (%)	Al (%)	O (%)	Zn/Co ratio
$CoAl_2O_4$	0	15.9	22.9	61.2	Zn_0Co_1
$Zn_{0.2}Co_{0.8}Al_2O_4$	3.2	13.3	22.4	61.1	$Zn_{0.19}Co_{0.81}$
$Zn_{0.4}Co_{0.6}Al_2O_4$	6.4	8.1	23.6	61.8	$Zn_{0.44}Co_{0.56}$
$Zn_{0.6}Co_{0.4}Al_2O_4$	7.9	5.8	21.9	64.4	$Zn_{0.58}Co_{0.42}$
$Zn_{0.8}Co_{0.2}Al_2O_4$	12.9	3.1	22.8	61.3	$Zn_{0.81}Co_{0.19}$
$ZnAl_2O_4$	14.6	0	22.6	62.8	Zn_1Co_0

Table S4. Specific surface areas of $Zn_xCo_{1-x}Al_2O_4$ determined by Brunauer-Emmett-Teller (BET) analysis of the N_2 adsorption/desorption isotherms in Fig. S4a and the average pore size determined by the Barrett–Joyner–Halenda method in Fig. S4b.

Sample	Surface area by BET analysis (m^2 g^{-1})	Average pore size (nm)
$CoAl_2O_4$	56.3	17.2
$Zn_{0.2}Co_{0.8}Al_2O_4$	43.8	24.8
$Zn_{0.4}Co_{0.6}Al_2O_4$	50.5	17.1
$Zn_{0.6}Co_{0.4}Al_2O_4$	46.8	19.8
$Zn_{0.8}Co_{0.2}Al_2O_4$	41.9	22.3
$ZnAl_2O_4$	29.8	29.3

Table S5. Curve fitting results of the electrochemical impedance spectroscopy (EIS) spectra in Fig. 2c using the equivalent circuit in Fig. S5.

Sample	R_1 (Ω)	R_2 (Ω)	Q_2 (μF·s $^{a-1}$)	a_2	R_3 (Ω)	Q_3 (μF·s $^{a-1}$)	a_3
$CoAl_2O_4$	4.165	120.2	0.047	0.973	5123	32.02	0.861
$Zn_{0.2}Co_{0.8}Al_2O_4$	4.719	93.74	0.038	0.996	8606	17.97	0.766
$Zn_{0.4}Co_{0.6}Al_2O_4$	1.752	54.73	0.158	0.949	7168	29.04	0.821
$Zn_{0.6}Co_{0.4}Al_2O_4$	1.708	55.82	0.175	0.932	1010	96.88	0.890
$Zn_{0.8}Co_{0.2}Al_2O_4$	3.423	101.1	0.068	0.961	6656	32.15	0.924
$ZnAl_2O_4$	2.767	119.2	0.081	0.937	66322	19.97	0.770

Table S6. Curve fitting results of X-ray photoelectron spectroscopy (XPS) spectra displayed in Figs. 4c and d for $Zn_{0.6}Co_{0.4}Al_2O_4$ before and after 1200 cycles of potential sweep between 0.926 V and 1.626 V vs. reversible hydrogen electrode (RHE) at a scan rate of 10 mV s^{-1}.

$Zn_{0.6}Co_{0.4}Al_2O_4$		Original	After 1200 cycles
Co $2p_{3/2}$	BE (eV)	781.3	781.6
	FWHM (eV)	4.2	3.3
	Area (%)	36.0	36.0
Co $2p_{3/2}$ sat.	BE (eV)	785.1	785.4
	FWHM (eV)	7.0	6.8
	Area (%)	30.7	30.7
Co $2p_{1/2}$	BE (eV)	797.2	797.5
	FWHM (eV)	4.4	3.8
	Area (%)	18.0	18.0
Co $2p_{1/2}$ sat.	BE (eV)	803.8	804.1
	FWHM (eV)	6.4	6.5
	Area (%)	15.3	15.3
O_L	BE (eV)	529.9	529.9
	FWHM (eV)	2.1	1.0
	Area (%)	29.8	1.0
O_D	BE (eV)	531.3	531.4
	FWHM (eV)	2.2	1.9
	Area (%)	22.5	63.2
O_A	BE (eV)	532.6	532.4
	FWHM (eV)	3.4	2.3
	Area (%)	47.69	35.7

*BE: binding energy; FWHM: full width at half maximum; OL: lattice oxygen; OD: oxygen defects; OA: adsorbed oxygen.

Table S7 concentration of cations in the 0.1 M KOH electrolyte of $Zn_{0.6}Co_{0.4}Al_2O_4$ after 1200 cycles of potential sweep between 0.926 V and 1.626 V vs. reversible hydrogen electrode (RHE) at a scan rate of 10 mV s^{-1}.

	Zn/ppm	Co/ppm	Al/ppm
Before 1200 cycles	0	0	0
After 1200 cycles	0.022	0.004	0.006